Outstanding Problems in Heliophysics: from Coronal Heating to the Edge of the Heliosphere
ASP Conference Series, Vol. 484
Qiang Hu and Gary P. Zank, eds.

Fe Enhancements in SEP Onsets: Flare/CME Mixture or Transport Effect?

G. M. Mason,[1] G. Li,[2] C. M. S. Cohen,[3] M. I. Desai,[4] D. K. Haggerty,[1] R. A. Leske,[3] R. A. Mewaldt,[3] and G. P. Zank[2]

[1]*JHU/Applied Physics Lab., Laurel, MD 20723, USA*
[2]*Department of Space Science/CSPAR, University of Alabama in Huntsville, Huntsville, AL 35899, USA*
[3]*California Institute of Technology, Pasadena, CA 91125, USA*
[4]*SouthWest Research Institute, San Antonio, TX 78828, USA*

Abstract. During the onset phases of SEP events, the Fe/O ratio is often observed to be initially enhanced (~1) over typical SEP values, followed by a decline to values close to typical averages over entire events (Fe/O ~0.1). Two mechanisms have been suggested to explain this behavior, namely (1) a two-step process with an initial injection of "flare" particles with high Fe/O followed by shock-accelerated particles with lower Fe/O, and (2) a transport effect wherein the lower charge-to-mass ratio of Fe vs. O results in faster transport of Fe to the observer, leading to enhanced Fe/O in the early stages of the event. Distinguishing between these two scenarios is important to building a basic picture of processes taking place in large SEP events. We have carried out a detailed study of 17 large SEP events where energetic particle data were fitted by a state-of-the-art model whose computed time-intensity profiles were compared to the observed profiles of H, He, O, and Fe over a very broad energy range. We find that the observed decrease in Fe/O during the rise phase can be reasonably fitted by the transport model where the differences in Fe vs. O transport are due to the slope of the turbulence spectrum of the interplanetary magnetic field (IMF).

1. Introduction

Decreases in the Fe/O ratio during solar energetic particle (SEP) event onsets are often observed (Scholer et al. 1978; von Rosenvinge & Reames 1979; Mason et al. 1983; Tylka et al. 1999) and attributed to a variety of processes such as the acceleration mechanism, shock geometry, mixtures of particle populations, and interplanetary transport (Scholer et al. 1978; von Rosenvinge & Reames 1979; Mason et al. 1983; Tylka et al. 1999; Reames et al. 2000; Li & Zank 2005; Tylka et al. 2005; Li et al. 2009a). Recently, several lines of evidence have shown that some energy dependence of particle abundances or temporal changes such as in the Fe/O ratio are lessened or largely removed if particles are compared not at the same energy/nucleon but rather when they have the same value of the diffusion coefficient (Cummings et al. 1984; Cohen et al. 2005; Mason et al. 2006). For example, in the case of solar energetic particle (SEP) Fe and O, this implies that particles should be compared at scaled energies, given by $E_O/E_{Fe} = [(Q/M)_O/(Q/M)_{Fe}]^{2\alpha/(\alpha+1)}$, where α is related to the spectral index $-q$ of interplanetary magnetic turbulence as $\alpha = 2 - q$ (Dröge 1994). For typical SEP charge to mass (Q/M) ratios and interplanetary turbulence spectral index of -5/3, the energy ratio is ~2. In order to explore whether this simple diffusive transport property is contained in a detailed model of interplanetary transport, we modified the transport model developed by the Huntsville group (Li 2008; Li et al. 2003, 2005) to include adiabatic deceleration and non-isotropic distribution functions and compared the calculations with observations of 17 large western hemisphere solar energetic particle events (Mason et al. 2012, hereafter Paper 1), and report here additional aspects of this study.

2. Observations And Model Fitting

Figure 1 shows particle spectrograms of $1/v$ arrival times of SEP heavy ions for 3 events in the survey and illustrates the great variety of behavior even for large western hemisphere events.

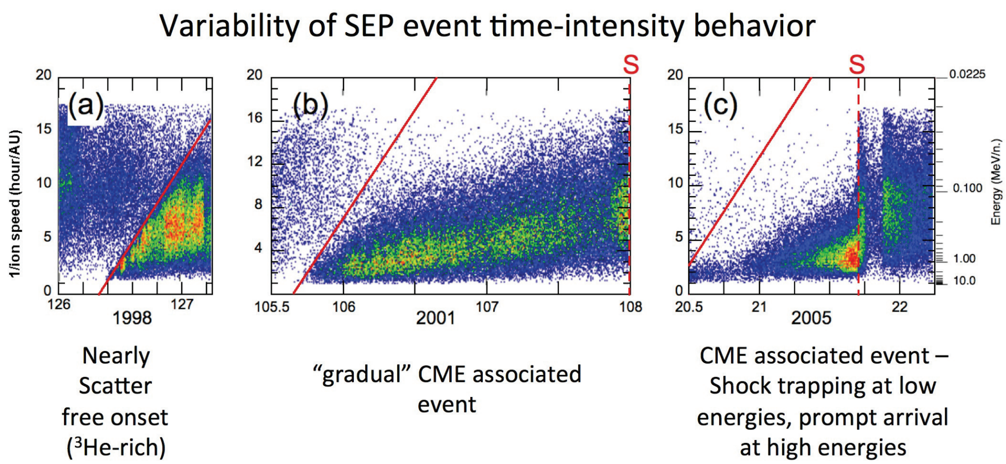

Figure 1. Ion arrival times for 3 SEP events, where red diagonal lines show the expected arrival time for direct transport down a 1.2 AU IMF line; (a) event with nearly scatter-free initial arrivals, (b) gradual event showing much delayed arrivals, and (c) event dominated by shock trapping where low energy particles appear to be trapped by the shock (in this event high energy particles arrived promptly). Figure adapted from Mason et al. (2012).

In the Paper 1 survey ~2/3 of events showed decreases in Fe/O during the rise phase, with others showing no temporal change or irregular variations. For 11 events showing Fe/O decreases, Figure 2 shows an epoch analysis at low and high energies, timed to start at the x-ray maximum of each event. The decrease in Fe/O during the initial rise in particle intensity is clearly present and largely disappears when Fe/O is computed at scaled energies.

To keep the number of free parameters in the model at a minimum, particles were given a delta-function injection at the x-ray maximum time. The model produced reasonably good fits to individual time-intensity profiles of H, He, O and Fe, over a range of ~0.5 MeV/nuc to >100 MeV/nuc where statistics permitted (see Paper 1). At energies below ~1 MeV/nuc, however, the profiles were often dominated by the shock, precluding low energy fits. Figure 3 shows the energy ranges over which shock associated particles dominated; not surprisingly, the events with the highest GOES >10

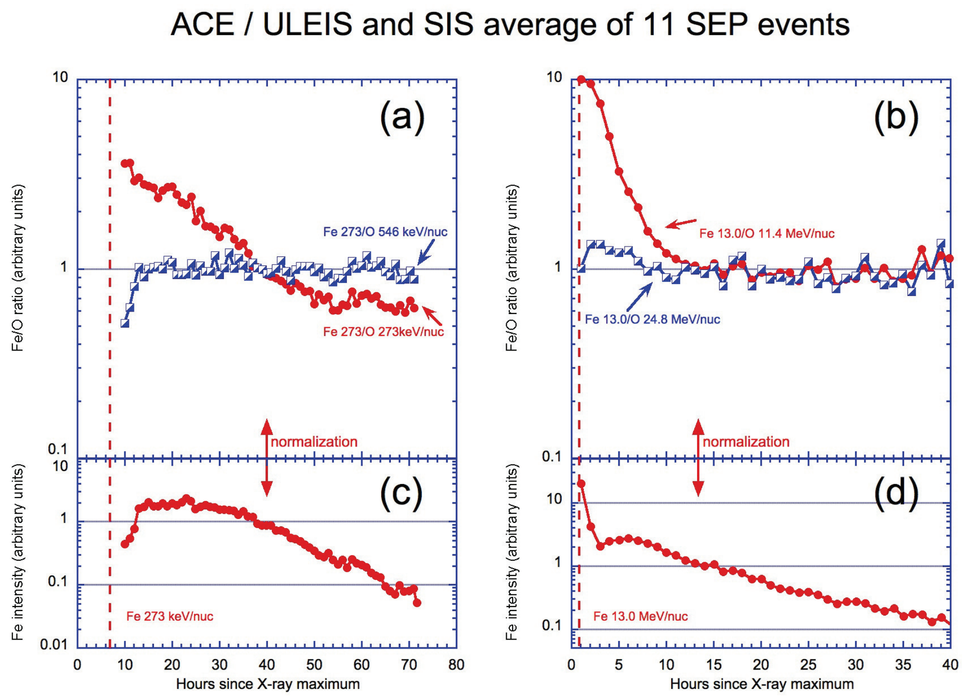

Figure 2. Red points: Fe/O decreases for 11 SEP events at (a) 273 keV/nuc and (b) ~12 MeV/nuc normalized to 1.0 at the time indicated. 1-hr average time-intensity profiles (c) and (d) also normalized at the times shown. The 11 events were logarithmically averaged after normalization to give a more nearly equal weighting to all events. Blue half-filled squares show that when compared at scaled energy, most of the temporal variation disappears. Dashed vertical red lines show direct flight time to Earth on a 1.2 AU spiral.

MeV proton maximum intensities tended to be those where the shock dominated to the highest energies.

Additionally, details of connection to the acceleration region sometimes gave irregular onset profiles (e.g., Figure 1(a) and Paper 1 Figure 4(b, d)) which were fitted only in a smoothed fashion. In about a third of the cases at low energies, and ~2/3 of the cases at high energies, the delta-function injection produced rises that were too fast and decays that had a reasonable time constant, but which occurred earlier than the observations. For these cases extended injections of the type $I = I_0 \exp(-t/\sigma_t)$ greatly improved the fits (Reid 1964; Beeck et al. 1987; Schulze et al. 1977). Values of $\sigma_t \sim 5hr$ worked in most cases, as can be seen from Figure 4 (left), and have been ascribed in previous studies to time scales of acceleration by the CME shock (Kahler 1994; Lee 2005); in a few cases σ_t up 10-15 hrs was needed (see Paper 1).

The right panel of Figure 4 shows the average scattering mean free path for the 17 fits, where we integrated the phase space diffusion coefficient over pitch angle following references Jokipii (1966); Hasselmann & Wibberenz (1970); Earl (1974); Bieber et al. (1994), although we note that other approaches might derive different mfp values for the same turbulence levels (Qin et al. 2006). The fitted average value $\lambda = 0.047P^{0.287}$ is similar to those found in previous studies (e.g., Bieber et al. 1994,

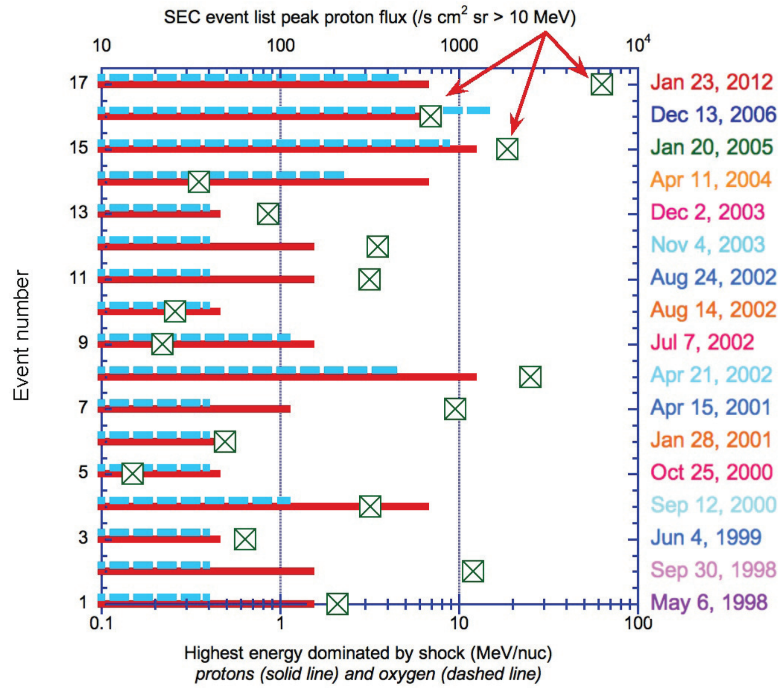

Figure 3. Energies below which shock associated particles dominated the proton (solid red lines) and oxygen intensity (dashed blue lines). Shocks dominated below ~0.5 MeV/nuc in all 17 events, while in the most intense events (squares with crosses) shock domination extended up to ~10 MeV for protons. Model fits were not made in energy ranges dominated by shocks.

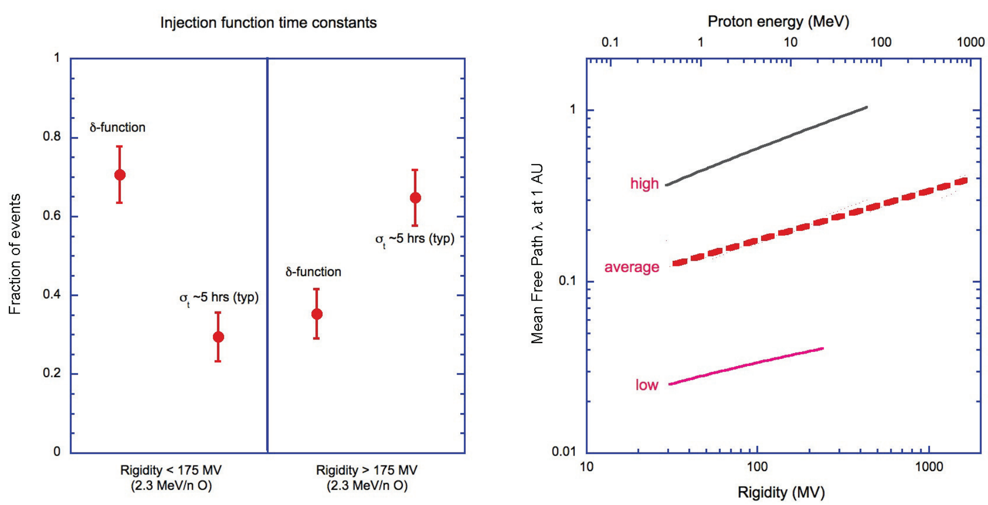

Figure 4. Left panel: injection time constants at low and higher energies used in fits. Right panel: average scattering mean free path for 17 fits, and as well as largest and smallest mean free path used.

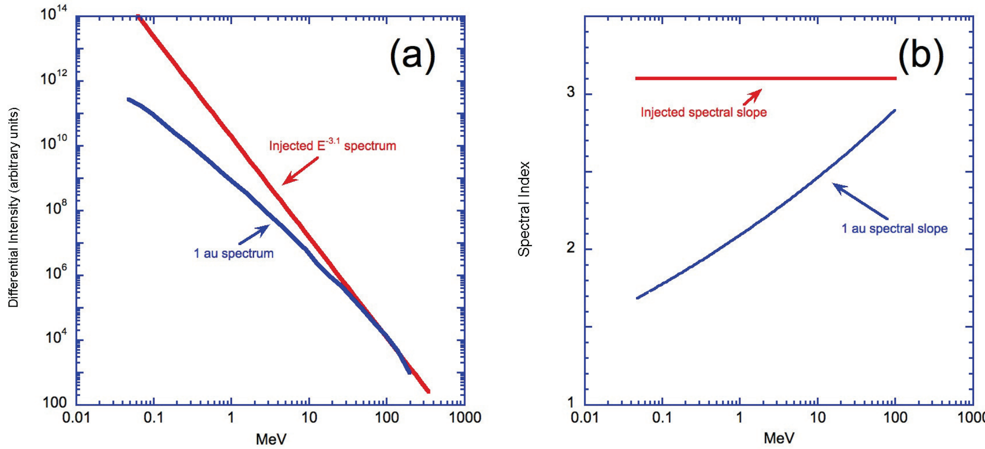

Figure 5. (a) injected and 1 AU spectrum showing greater spectral rollover at low energies due to adiabatic deceleration, but no spectral "break". (b) spectral index of injected (upper line) and 1 AU (lower line) spectra.

and references therein). The largest and smallest values are also shown in the figure; the event with the highest λ (Aug. 14, 2002) showed nearly scatter free arrival of particles similar to that shown in Figure 1(a). The SEP events where there was no decrease in Fe/O during the rise phase were fitted with turbulence index q = -1.9 which gives an energy shift of ~0 (see Paper 1 for details).

Paper 1 describes the effect of adiabatic deceleration computed with the model, where it was found that for typical events particles injected at the Sun at ~1 MeV/nuc arrived at 1 AU with their energies greatly smeared out, and those injected below 200 keV/nucleon were sufficiently cooled as to be unobservable at 1 AU. It is natural to ask if this energy dependence could lead to the often observed spectral breaks in ion spectra (Cohen et al. 2005; Mewaldt et al. 2005). Figure 5 shows a sample calculation for an $E^{-3.1}$ injected spectrum at the Sun. Adiabatic deceleration causes increasing rollover towards low energies, however, this change is quite smooth and does not resemble the observed "breaks" which generally occur over a relatively narrow range with power law spectra on either side. To create such a feature in our model would require a distinct change in the transport coefficients in the range of the break, which is not present in our assumed form of the interplanetary turbulence. In order to fit the observed spectra in our events, spectral breaks were put into the injected spectrum (see Paper 1 for details). Consequently, one may attribute the break as a feature of acceleration. Indeed, Li et al. (2009b) have used the (Q/M) dependence of the break energy to infer the shock geometry when these particles are accelerated near the Sun.

Figure 6 shows that Fe/O ratios from the simulation exhibit the same temporal properties seen from the epoch analysis in Figure 2(a) and (b), namely an order of magnitude decrease in Fe/O calculated at the same energy/nucleon, compared with a nearly flat ratio when the O energy is scaled. The similarity of the simulation and observations is clear, and this is also seen in the event-by-event comparisons shown in Paper 1 which, however, show that in some events the timing of the decrease differs from the simulation presumably due to connection or particle release effects. An additional feature, shown in Paper 1 is that the particle transport model predicts that the O/He ratio

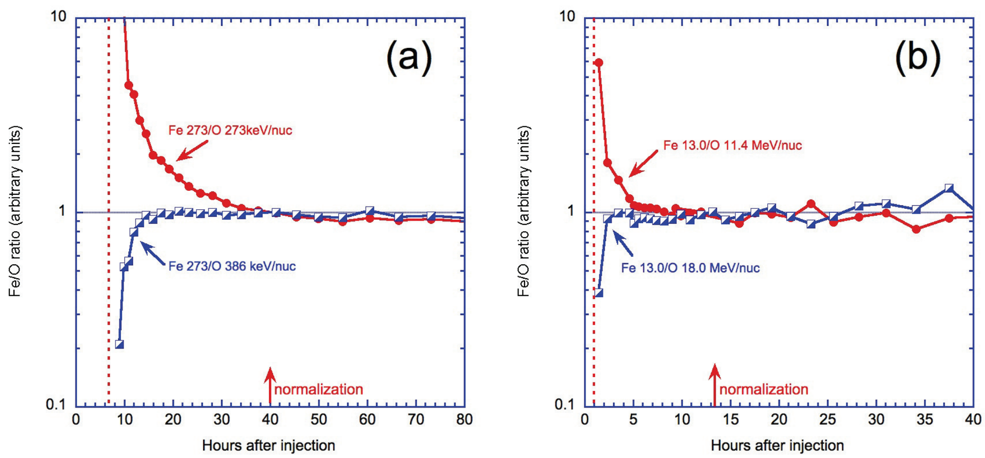

Figure 6. (a) simulated low energy Fe/O ratio at 386 keV/nuc (filled circles) and at scaled energy (half filled squares) showing removal of most energy dependence at scaled energies. (b) same as (a) except for 13.0 MeV/nuc. Initial rise in scaled Fe/O is due to earlier arrival of Fe nuclei whose first arrivals have undergone little scattering on way to 1 AU.

should also show time variations since SEP O is not fully stripped. Such a variation would not be predicted if the Fe/O decrease were due to a mixture of "flare" and CME-accelerated material since "flare" O/He in ^{3}He-rich events shows the same O/He ratio as CME-accelerated material (see Paper 1 for details).

3. Conclusion

We have carried out a study of 17 western hemisphere SEP events using a detailed model of SEP propagation in order to investigate if the energy scaling feature which largely removes Fe/O ratio decreases during SEP event onsets can be fitted with a detailed transport model. We find that the energy scaling property is preserved in the detailed model. Energy scaling can be qualitatively understood as being due to the diffusion coefficient organizing the data, rather than particle speed, and also plays a role in organizing particle energy spectra as well as timing characteristics in those events where interplanetary scattering is significant. Physically, the energy scaling arises from the *slope* of the interplanetary magnetic field turbulence spectrum and the differing charge-to-mass ratios of SEP ions. An important prediction of the model, that O/He will show similar behavior to Fe/O, was confirmed and is not predicted in particle mixture scenarios. These considerations do not rule out the possibility e.g., of SEP event types or seed particle mixtures causing Fe/O time variations, but given the properties of particle transport, ionization states of SEP ions, and the IMF turbulence spectrum, we conclude that transport is the cause of these variations in most cases.

Acknowledgments. This work was supported by NASA under LWS TR&T grant NNX07-AP69G (APL), and other grants including NNX09AP74A (UAH), NNX08AI11-G (Caltech), and NNX08AK87G (SwRI) and NSF grants including AGS-1135432 (UAH) and ATM-0551127 (SwRI). Figure 1 is reproduced by permission of the AAS.

References

Beeck, J., Mason, G. M., Hamilton, D. C., Wibberenz, G., Kunow, H., Hovestadt, D., & Klecker, B. 1987, ApJ, 322, 1052
Bieber, J. W., Matthaeus, W. H., Smith, C. W., Wanner, W., Kallenrode, M.-B., & Wibberenz, G. 1994, ApJ, 420, 294
Cohen, C. M. S., Stone, E. C., Mewaldt, R. A., Leske, R. A., Cummings, A. C., Mason, G. M., Desai, M. I., von Rosenvinge, T. T., & Wiedenbeck, M. E. 2005, Journal of Geophysical Research (Space Physics), 110, A09S16
Cummings, A. C., Stone, E. C., & Webber, W. R. 1984, ApJ, 287, L99
Dröge, W. 1994, ApJS, 90, 567
Earl, J. A. 1974, ApJ, 188, 379
Hasselmann, K., & Wibberenz, G. 1970, ApJ, 162, 1049
Jokipii, J. R. 1966, ApJ, 146, 480
Kahler, S. 1994, ApJ, 428, 837
Lee, M. A. 2005, ApJS, 158, 38
Li, G. 2008, in American Institute of Physics Conference Series, edited by G. Li, Q. Hu, O. Verkhoglyadova, G. P. Zank, R. P. Lin, & J. Luhmann, vol. 1039 of American Institute of Physics Conference Series, 233
Li, G., Webb, G. M., le Roux, J. A., Wiedenbeck, M., Florinski, V., & Zank, G. P. 2009a, in International Cosmic Ray Conference, vol. 31 of ICRC, 1
Li, G., & Zank, G. P. 2005, Geophys. Res. Lett., 32, L02101
Li, G., Zank, G. P., & Rice, W. K. M. 2003, Journal of Geophysical Research (Space Physics), 108, 1082
— 2005, Journal of Geophysical Research (Space Physics), 110, A06104
Li, G., Zank, G. P., Verkhoglyadova, O., Mewaldt, R. A., Cohen, C. M. S., Mason, G. M., & Desai, M. I. 2009b, ApJ, 702, 998
Mason, G. M., Desai, M. I., Cohen, C. M. S., Mewaldt, R. A., Stone, E. C., & Dwyer, J. R. 2006, ApJ, 647, L65
Mason, G. M., Gloeckler, G., & Hovestadt, D. 1983, ApJ, 267, 844
Mason, G. M., Li, G., Cohen, C. M. S., Desai, M. I., Haggerty, D. K., Leske, R. A., Mewaldt, R. A., & Zank, G. P. 2012, ApJ, 761, 104
Mewaldt, R. A., Cohen, C. M. S., Mason, G. M., Labrador, A. W., Looper, M. L., Haggerty, D. E., Maclennan, C. G., Cummings, A. C., Desai, M. I., Leske, R. A., Li, G., Mazur, J. E., Stone, E. C., & Wiedenbeck, M. E. 2005, in The Physics of Collisionless Shocks: 4th Annual IGPP International Astrophysics Conference, edited by G. Li, G. P. Zank, & C. T. Russell, vol. 781 of American Institute of Physics Conference Series, 227
Qin, G., Matthaeus, W. H., & Bieber, J. W. 2006, ApJ, 640, L103
Reames, D. V., Ng, C. K., & Tylka, A. J. 2000, ApJ, 531, L83
Reid, G. C. 1964, J. Geophys. Res., 69, 2659
Scholer, M., Hovestadt, D., Klecker, B., Gloeckler, G., & Fan, C. Y. 1978, J. Geophys. Res., 83, 3349
Schulze, B. M., Richter, A. K., & Wibberenz, C. 1977, Solar Phys., 54, 207
Tylka, A. J., Cohen, C. M. S., Dietrich, W. F., Lee, M. A., Maclennan, C. G., Mewaldt, R. A., Ng, C. K., & Reames, D. V. 2005, ApJ, 625, 474
Tylka, A. J., Reames, D. V., & Ng, C. K. 1999, Geophys. Res. Lett., 26, 2141
von Rosenvinge, T. T., & Reames, D. V. 1979, in International Cosmic Ray Conference, vol. 5 of ICRC, 68